Bright Fission: Singlet Fission into a Pair of Emitting States

David Casanova*

Kimika Fakultatea, Euskal Herriko Unibertsitatea (UPV/EHU) and Donostia International Physics Center (DIPC), P.K. 1072, 20080 Donostia, Euskadi, Spain

IKERBASQUE, Basque Foundation for Science, 48013 Bilbao, Euskadi, Spain

Ⓢ Supporting Information

ABSTRACT: This paper reintroduces and explores the generation of two bright states from a single photon via a singlet fission mechanism in organic materials. This particular photophysical process is labeled here as bright fission (BF). The central part of the study is devoted to set the theoretical foundations of BF by discussing possible electronic mechanisms, the role of different excited states with various physical nature, the presence of competing deactivation channels, and the possible requirements for the BF viability. In a second part, some of the properties related to BF are computationally explored in anthracene. The analysis of computed high-lying excited states identifies several optical transitions as good candidates to trigger BF in anthracene. The approximation of excitonic couplings of these high energy levels to other electronic states within the same energy range suggests possible paths to populate electronic configurations potentially able to split in two independent spin singlets, i.e. singlet–singlet states. The study also explores the electronic structure of the energetically lowest singlet–singlet states in anthracene dimers and discusses the presence of charge transfer configurations and their relation to the singlet–singlet manifold. The computational results suggest fast relaxation to the lowest singlet–singlet state, from which the excitonic fission may occur. All in all, the present work aims at motivating to pursue further efforts in the study of the BF process in organic materials.
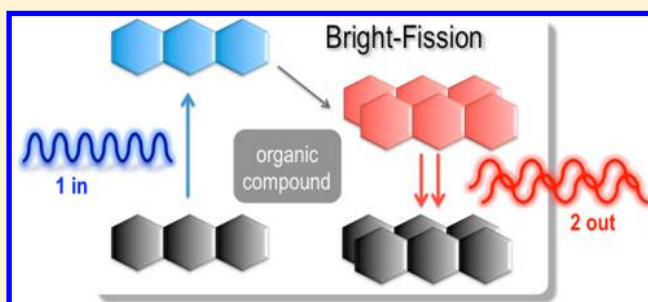
1. INTRODUCTION

1.1. Singlet Fission. Singlet fission (SF)[1,2] is a special example of internal conversion between electronic states with the same multiplicity of spin. In the literature, SF refers to the conversion of an excited singlet state into two triplet states in organic chromophores. The simplest and general description of SF is given by eq 1, where S_0 and S_1 are the ground and first excited singlet states, and T_1 is the lowest triplet of a chromophore.

$$S_0 + S_1 \rightleftharpoons T_1 + T_1 \qquad (1)$$

This process was discovered nearly 50 years ago,[3] but it was not until 2004 that Nozik et al.[4] suggested that the exciton multiplication in SF could be used to surpass the Shockley-Queisser theoretical limit of single-junction solar cells[5] and improve in this way the efficiency of photovoltaic devices. Since then the interest toward SF has grown very rapidly, and it has become one of the most promising multiexciton generation (MEG) mechanisms for solar energy conversion.[6-16]

In the past decade many experimental efforts have provided key insight for a better understanding of the SF phenomenon, detecting SF in a variety of organic compounds[17-23] and different structural morphologies,[24-28] measuring improved efficiencies,[29,30] determining the key parameters to improve SF rates,[31-35] or integrating SF materials in photovoltaic cells.[7,15,36,37] Simultaneously, these works have been very nicely complemented by major theoretical advances in the field.[1,2] In particular, theoretical models and computational studies have unveiled important details regarding the electronic states involved,[38-41] exploring their energies and couplings,[42-44] or suggesting possible mechanisms and their kinetics.[11,45-52]

1.2. Bright Fission. The final product of the SF reaction corresponds to two spin triplet excitons that in the case of purely organic materials typically have very low emission efficiencies (dark states). Instead, if the exciton fission could eventually result in two bright states it would enormously expand the range of applicability of such type of phenomenon. Two possible paths might be devised in order to employ exciton fission mechanisms for the emission of two photons from a higher frequency incident radiation: (i) transferring the generated triplet excitons from the singlet fission material to a phosphorescence emitter, for instance to an inorganic or organometallic compound, and (ii) the singlet exciton fission into a pair of fluorescent singlet states. The former strategy relies on the combination of two systems, a SF material and a compound with efficient phosphorescence capability, while the latter invokes a different photophysical reaction than the one involved in the SF process. The present study focuses on the transition of a high-energy exciton into two lower spin-singlet states. In the following this phenomenon will be labeled as BF

(Bright Fission) to be distinguished from the fission process yielding two triplets (SF).

In addition to the potential use as a MEG mechanism in photovoltaics like SF, the generation of two fluorescence emission events from each absorbed photon in purely organic materials could have a tremendous impact in lighting applications. Quantum efficient luminescent materials present great interest for their potential use in a variety of technologies, such as lasers, LED, plasma displays, detectors, and bioimaging as well as in photovoltaics.[53−55] One of the most appealing routes to reach the desired efficiencies relies on the idea of down-converting incident high-energy photons to two or more low-energy photons. In inorganic materials this phenomenon is known as quantum cutting and has been especially successful in the case of rare earth compounds[56] due to the presence of a large number of accessible energy levels. The discovery of BF materials would allow building organic thin films replacing expensive, narrow line-width inorganic materials with cheap, broadly absorbing organic compounds.

At this point, however, the foundations of BF remain unknown. Although the fission into a pair of singlet states process was already proposed in 1975 as a bimolecular deactivation channel for high-energy states in crystalline anthracene,[57] it has remained largely unexplored ever since. As far as I am aware of, neither experimental nor theoretical efforts have been pursued in order to understand the fundamentals of such phenomenon. Only on very few occasions this photoinduced conversion has been mentioned.[58−60]

1.3. Objectives. The present paper aims at reintroducing a forgotten photophysical process, that is the fission of a singlet state into a pair of fluorescent states, and to develop initial theoretical guidelines for further developments. With this general goal in view, this work proposes and discusses possible mechanisms for the BF process and its feasibility, electronic states directly or indirectly involved in BF, competing exciton deactivation channels and lists the requirements and key factors controlling its efficiency.

Furthermore, this study aims to motivate investigations on this phenomenon, both experimentally and at the theoretical and computational level. More specifically, the first step toward advancing in the study of BF should be addressed to revisit the experiment carried out by Klein and Voltz[57] in order to verify and improve its measurements on the BF feasibility in anthracene.

2. THEORY

2.1. Generalities. The general reaction for the BF process can be represented by the simplified kinetic scheme shown in eq 2. Following a bimolecular model analogous to the one commonly employed in SF,[1] it might be anticipated that the BF conversion process relies on the formation of an intermediate precursor state corresponding to an interacting pair of singlet excitons located on two adjacent chromophores (SS), that is two molecules in the case of molecular materials or aggregates, or two molecular fragments in polymers or covalent dimers. In a second step, the SS state decouples in two excitons with the potential ability to photoemit (bright states). Therefore, the BF kinetics can be divided in two parts: (i) the formation of the SS state and (ii) its dissociation into two independent singlets. The possible diffusion of the generated singlets through the material and the eventual fluorescence emission should be also considered as part of the overall BF process.

$$S_0 + S_n \rightleftharpoons {}^1(SS) \rightleftharpoons S_1 + S_1 \qquad (2)$$
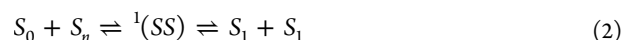
Alternatively, the BF electronic process in eq 2 can be also interpreted as the inverse mechanism of the singlet−singlet exciton fusion,[61] that is the annihilation of two singlet excitons to a higher singlet state, observed in organic molecular materials exposed to high-intensity radiation.[62]

The existence of an accessible SS state with the convenient properties, such as relative energy and electronic coupling to other excitons or spatial delocalization, are of great relevance and ultimately will determine the fate of BF. The electronic structure of SS is, by definition, of mutiexcitonic nature, with energies expected to lie in the order of the sum of two independent excitons, at least for weakly interacting chromophores. The energy cost for the generation of two singlet excitons in organic compounds will be, in general, considerably higher than the energy threshold necessary to trigger the SF process (twice the energy of the lowest triplet state). These energy requirements might pose a tough impediment to controlled BF experiments. In addition, the detection and measurement of BF also poses some difficulties. The direct detection of BF could be attained by measuring the rate of emitted versus absorbed photons. The presence of BF might be univocally detected by fluorescence yields over 100%, but other techniques typically used in the study of SF might be less practical. For instance, in BF all single and multiple excitonic (ME) states hold singlet spin multiplicity, hence magnetic field effects cannot be employed to indirectly detect the presence of the BF processes. In SF, it is common to perform time-resolved experiments looking for the simultaneous decay of the excited singlet state and an increase in the population of the triplet state by means of transient absorption spectroscopy; but such type of experiments are expected to be less useful in BF, due to the fact that the fission process relaxes to the same excitonic state (S_1) as the relaxation through the single exciton manifold via internal conversion (IC).

2.2. Electronic States Related to BF. The understanding of BF involves the study of a variety of excited states, which may hold differences in their electronic nature. From the general equation for the BF reaction (eq 2) it becomes evident that, in addition to the ground state, at least three other spin singlet states, S_1, S_n, and SS, are directly involved in the BF phenomenon, but additional states not shown explicitly in eq 2 could also be either directly or indirectly related to BF.

2.2.1. Optical States. The first populated exciton (S_n) is of vital importance, since it will dictate the manifold of accessible states following the initial transition. In the case of photoexcitation S_n must be optically active, and its availability will strongly depend on the frequency of the incident photons. In fact, it might be advisable to consider several optical states, especially in the case of high-energy incident radiation.

2.2.2. Emitter States. The lowest excited singlet is the final product of the BF reaction, and in order for the whole process to generate two low energy photons, the de-excitation of S_1 to the ground state must be dipole allowed (radiative decay). Although less probable, for some compounds it might be also possible to photoemit from a higher excited states S_i, $i > 1$.

2.2.3. Multiexciton SS State. The availability of the fission of an excited state into two bright states relies on the idea of the existence of a precursor state that can be described as the coupling of two singlet excitons. In the case of a molecular material or aggregate this could be seen as a biexcited state formed by two spin-singlet single excitations in adjacent

chromophores. Hence, like in the SF precursor state, the BF precursor is expected to hold ME character and, to the very least, be delocalized over two chromophoric moieties. In fact, we can imagine an entire family of ME states with the general form S_iS_j corresponding to the coupling of S_i and S_j spin-singlet single excitations on two monomers. Typically, for weakly interacting chromophores, such as molecular crystals, aggregates or weakly coupled covalent dimers, the lowest energy state within the S_iS_j manifold is expected to be formed by the pair of the lowest excited singlets of each of the monomers, i.e. the S_1S_1 state. Therefore, as a first approximation, the electronic structure of the S_1S_1 exciton can be expressed as the direct product between two S_1 states. In this sense, I consider here the precisely defined (diabatic) $|S_1S_1\rangle$ state as $|S_1S_1\rangle \equiv |S_1\rangle \otimes |S_1\rangle$. If the $|S_1S_1\rangle$ is approximated in terms of the highest occupied molecular orbital (HOMO) and lowest unoccupied molecular orbital (LUMO) of each of the two coupled chromophores, its mathematical expression results in a linear combination of doubly excited configurations with four unpaired electrons occupying the four frontier orbitals as shown in eq 3

$$|S_1S_1\rangle \approx \frac{1}{2}|h_A h_B l_A l_B|(\alpha\alpha\beta\beta + \beta\beta\alpha\alpha - \alpha\beta\beta\alpha - \beta\alpha\alpha\beta)$$

(3)

where h and l correspond to HOMO and LUMO, A and B subindices indicate different monomers, and α and β are the $m_s = 1$ and -1 spin functions, respectively. Within this simple approach, the energy of the S_1S_1 state can be formulated as twice the energy of the lowest singlet of the monomer ($E(S_1)$) slightly shifted by the intermolecular interaction between the two singlet excitons (eq 4)

$$E(S_1S_1) = 2E(S_1) + K_{h_A l_B} - \frac{1}{2}\left(K_{h_A h_B} + K_{l_A l_B}\right)$$

(4)

where K is the exchange integral between orbitals of different monomers in the dimer. Hence, in the case of weakly interacting chromophores, the energy shift with respect to $2E(S_1)$ is expected to be rather small.

Analogously, the electronic structure of other S_iS_j states might be generally expressed by the linear combination of direct products between S_i and S_j states on the two monomers, $|S_iS_j\rangle \equiv c_{ij}|S_i\rangle \otimes |S_j\rangle + c_{ji}|S_j\rangle \otimes |S_i\rangle$, where $|c_{ij}|^2 + |c_{ji}|^2 = 1$. Asymmetry between c_{ij} and c_{ji} coefficients will arise in the case of heterodimers or as the result of nonsymmetric disposition of homodimers.

2.2.4. Charge Transfer and Charge Resonance States. Excitonic electronic states with strong ionic character, i.e. charge resonances (CR), or true intermolecular electronic transitions, i.e. charge transfer states (CT), are expected to have a significant influence on BF. Although the presence of CT states as intermediates seems very likely from a mechanistic point of view in SF, it is worth mentioning that in many cases the lowest CT configurations only act (at best) as indirect partners in SF, because they lie too high in energy as compared to $2E(T_1)$.[42,44] This is not expected to be the case in BF. The energy of the BF precursor is much higher than in SF, that is $2E(S_1) \gg 2E(T_1)$. Hence CR and/or CT states are expected to play a significant role in BF processes. Actually, it is not obvious whether they would enhance the BF rates or their participation would induce a decrease of total fission events. This point will be discussed in detail for the anthracene dimer case study in section 3.

The number and variety of states that might participate in BF suggest that the BF deactivation of the initially photoexcited exciton might follow a more complex mechanism than the one described by the two-step reaction in eq 2, as indicated in the Jablonski diagram shown in Figure 1.

Figure 1. Jablonski diagram with proposed potential BF mechanisms. A, absorption; IC, internal conversion; MEF, multiexciton formation; ED, exciton dissociation; F, fluorescence.

2.3. Competing Deactivation Channels. Ultimately, the feasibility of BF depends on the relative ratio with respect to other possible relaxation pathways from the photoactivated state. Therefore, it is mandatory to be aware of the alternative available deactivation channels in competition with BF. Some of the interfering reactions with the BF process could be as follows:

(i). Decay to the Lowest Exciton. Probably the most efficient channel blocking BF is the system's relaxation within the Frenkel manifold down to the lowest excited (bright) singlet state, with the final emission of a single photon. The decay to S_1 is expected to be relatively fast compared to other channels as pointed by the success of Kasha's rule[63] in describing the relaxation processes in many systems.

(ii). Singlet–Singlet Annihilation. Even in the case of the successful generation of two bright states via a BF mechanism, if the back reaction, i.e. the fusion of two excited excitons, is fast, it will result in no net production of fission singlets.

(iii). Ionization. The need to promote the absorbing system at the very least to twice the energy of the bright state could produce the ionization of the system. In fact, the ionization potential of some typical organic chromophores is in many cases in the order of $2E(S_1)$.[64] Even in the case of no resonant ionization due to photoabsorption, some high-lying states could eventually trigger autoionization mechanisms blocking the BF process.

(iv). Nonradiative Relaxation of S_1. Obviously, in addition to generation of two single excitons, the definition of BF implies that these must decay radiatively. Therefore, efficient IC to the ground state, intersystem crossing (ISC), or even the fission to two triplet state (SF) must be avoided if we aim to design luminescence materials. The rate of nonradiative $S_1 \rightarrow S_0$ IC is related to the energy gap between the two states. Small gap increases the probability of radiationless transition.[65,66] ISC and SF of S_1 to the triplet manifold of states are two other possible fluorescence emission suppressing mechanisms. Although it might be difficult to control the presence of triplet states with energies $\leq 2E(S_1)$, ISC is commonly a rather slow process in organic materials.

2.4. Requirements for Efficient BF. This section summarizes all the points previously discussed regarding the

electronic states, possible mechanisms, and competing channels and highlights the most important parameters and characteristics for a system to undergo BF.

(i). Thermodynamic. To ensure exoergic BF, the transition energy to the photoexcited state (S_n) must be at least twice the energy of the lowest excited singlet (S_1): $E(S_n) \geq 2E(S_1)$. Therefore, it is necessary the existence of a highly absorbing optical S_n state at this energy range.

(ii). Kinetic. The BF competes with other relaxation mechanisms; therefore its efficiency depends on the relative rates of these competing processes. Thus, it is necessary a fast formation of the ME precursor state. The *SS* manifold might be directly reached: (a) via nonadiabatic coupling from S_n, (b) through an intermediate state, which might have either excitonic or CT character, or (c) by coherent population, as it has been recently identified as a possible mechanism for the formation of the *TT* state in pentacene.[31,35,40] For a fast nonadiabatic transition to the singlet–singlet ME manifold there must exist a S_m state ($m \leq n$) with an energy close to the sum of two singlets of the monomer, S_i and S_j with $i, j \geq 1$: $E(S_m) \sim E(S_i) + E(S_j)$. In the case of BF mediated by a CT intermediate, it will be necessary that $E(S_m) \sim E(S_+) + E(S_-)$. On the other hand, the coherent mechanism requires effective overlap between optical and ME states at the excitation energy.

(iii). Chromophore Coupling. The electronic coupling between chromophores has a direct effect on the relative efficiency of the ME generation and subsequent fission with respect to other deactivation channels. In order to access the manifold of singlet–singlet states through nonadiabatic transition from one or more Frenkel states, it is necessary to have large nonadiabatic couplings (NAC) between S_m ($m \leq n$) and S_iS_j, with $i, j \geq 1$. Once S_iS_j is populated, it can return back to a Frenkel exciton via IC before the fission takes place. Hence, it is convenient to have small NAC between *SS* states and molecular excitations with energies below $E(S_iS_j)$. The efficient fission of the ME state into two independent excited singlets requires that $E(S_iS_j) \geq E(S_i) + E(S_j)$, which suggests weak coupling between chromophores. Therefore, as in the case of SF, aggregates and molecular crystals should be good candidates for BF processes. Efficient BF in dimers or oligomers could be also obtained by singlet–singlet decoupling via intramolecular motion following some relaxation mode. The cost of the singlet–singlet dissociation in BF can be measured as the energy difference $E(S_iS_j) - E(S_i) - E(S_j)$.

It is also important to bear in mind that, the feasibility of the BF mechanism (or mechanisms) will not only depend on the specific photophysical properties of each material, but it might also be linked to the experimental conditions such as the excitation energy, the intensity of the incident radiation, and the temperature of operation.

3. A CASE OF STUDY: ANTHRACENE

In the following I will study some aspects related to the BF process in anthracene. First I will explore possible paths to populate the *SS* manifold. Then, I will characterize and discuss the electronic structure properties of the lowest *SS* states as possible BF precursors. Finally, I will investigate some aspects regarding the spatial nature of the optical excitons. A full discussion of low- and high-lying excited states of the anthracene molecule and the computational methodologies employed in the present study can be found in the Supporting Information.

3.1. Population of the SS Manifold. In this section I explore the direct transition from a photopopulated S_n state to energetically close S_iS_j composite states. For that purpose, I consider the two distinct molecular dimers between first neighbors present in the crystal structure of anthracene (Figure 2) as molecular models for the study of BF. All values presented
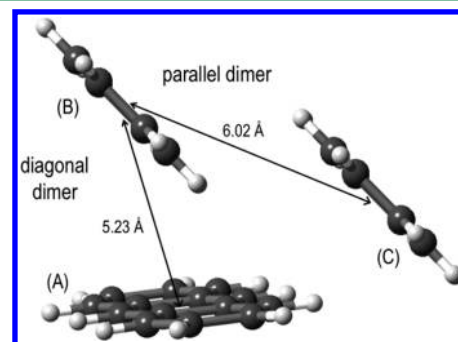
Figure 2. First neighbor molecular dimers in anthracene crystal considered in this work. A, B, and C labels are used to identify different monomers within a dimer (see discussion).

in this section have been computed within the TDDFT methodology with the M06 energy functional[67] and the 6-31+G(d,p) basis set.

The golden rule for the exciton transition assumes that the rate of the process is proportional to the square of the interstate coupling.[68] For the case of molecular dimers, the excitonic transition between a high-lying optical state to a *SS* multi-exciton can be modeled as $S_0S_n \rightarrow S_iS_j$, where S_0S_n corresponds to an exciton S_n localized on one molecule and S_iS_j labels the composite *SS* state delocalized on the entire dimer and characterized as the combination of S_i and S_j states. The classical approximation for this coupling can be expressed by the dipole–dipole Coulomb interaction between the molecular transition dipoles[69]

$$\langle S_0S_n|\hat{H}|S_iS_j \rangle \approx \frac{\vec{\mu}_{0i}\vec{\mu}_{nj}}{R^3} \tag{5}$$

where the left-hand side corresponds to the electronic coupling between the two states, $\vec{\mu}_{0i}$ and $\vec{\mu}_{nj}$ are the transition dipole moments between S_0 and S_i and between S_n and S_j, respectively, and R is the distance between the two molecules. Notice that if S_n is restricted to optically allowed states, it belongs to u-symmetry. In addition, eq 5 limits S_i and S_j to u and g-symmetric representations of D_{2h}, respectively.

The dipole–dipole interaction couplings (eq 5) between S_0S_n and S_iS_j states considering four possible initial excitations (S_n), 6^1B_{2u}, 8^1B_{2u}, 12^1B_{2u}, and 11^1B_{3u}, with excitation energies 6.67, 7.77, 8.12, and 8.13 eV (Table S1), are shown in Figure 3 as a function of the energy difference $E(S_i) + E(S_j) - E(S_0) - E(S_n)$. The diagonal dimer exhibits a larger variety of nonzero couplings than its parallel counterpart, in particular at small energy gaps. When the system is promoted to the first of these optical states ($S_n = 6^1B_{2u}$) there is basically no interaction of S_0S_n with the *SS* manifold, at least with S_iS_j states energetically close. The main couplings appear for $S_n = 8^1B_{2u}$ and 11^1B_{3u}, in particular for the latter. On the other hand, the Rydberg character of 12^1B_{2u} reduces the transition dipole interaction to g-symmetry valence states. The 11^1B_{3u} state has relatively large couplings to $1^1B_{2u}1^1B_{1g}$ and $1^1B_{2u}2^1B_{1g}$, which lie 0.18 and 0.35 eV below, respectively. In addition, the diagonal dimer shows
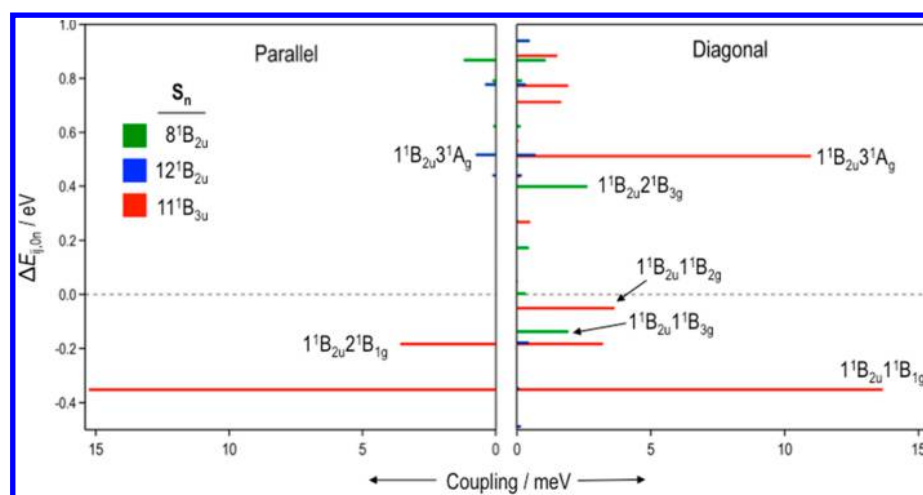
Figure 3. Energy gap between S_iS_j and S_0S_n ($\Delta E_{ij,0n} = E_i + E_j - E_0 - E_n$) vs absolute exciton coupling for the parallel (left) and diagonal (right) anthracene dimers computed as the Coulomb interaction in the dipole−dipole approximation (eq 5). Green, blue, and red horizontal bars correspond to $S_n = 8^1B_{2u}$, 12^1B_{2u}, and 11^1B_{3u}, respectively. Horizontal gray dashed line correspond to the S_0S_n energy, while labels for the largest couplings indicate the nature of the S_iS_j states.

several couplings in the vicinity of 5 meV at energies just below the S_0S_n level, corresponding to $1^1B_{2u}1^1B_{3g}$ ($S_n = 8^1B_{2u}$) and $1^1B_{2u}1^1B_{2g}$ ($S_n = 11^1B_{3u}$). The diagonal arrangement also induces important interaction to higher composite states (0.4−0.5 eV above $E(S_n)$), i.e. $1^1B_{2u}2^1B_{3g}$ dimer state for $S_n = 8^1B_{2u}$, and for $S_iS_j = 1^1B_{2u}3^1A_g$ and $S_n = 11^1B_{3u}$. These results are in agreement with experimentally observed qualitative increase of the BF efficiency in anthracene at the incident radiation of 8.2 eV and higher ones.[57]

3.2. Low-Lying *SS* States. The four lowest *SS* states can be labeled as combinations of the two lowest molecular excited singlets, i.e. 1^1B_{2u} and 1^1B_{3u} states (Table S1). Their computed excitation energies, multiexcitonic character, and CT mixings are presented in Table 1. All results presented in this section have been obtained at the restricted active space configuration interaction (RAS-CI)[70−72] level with the 6-31G(d) basis set. The RAS-CI computed energies have been corrected in order

Table 1. Excitation Energies, Multiexcitonic (ME), and Charge Transfer (CT) Contributions (in %), and Number of Unpaired Electrons (N_U) for the Parallel and Diagonal Anthracene Dimers Computed at the RAS-CI/6-31G(d) Level[a]

S_iS_j	character	energy	%ME	%CT	N_U
parallel dimer					
S_1S_1	$1^1B_{2u} \otimes 1^1B_{2u}$	6.63	97.6	1.1	4.08
S_1S_2 (+)	$1^1B_{2u} \otimes 1^1B_{3u}$	6.85	98.9	0.9	4.06
S_1S_2 (−)	$1^1B_{2u} \otimes 1^1B_{3u}$	6.86	98.8	0.9	4.06
S_2S_2	$1^1B_{3u} \otimes 1^1B_{3u}$	7.08	99.6	0.4	4.05
diagonal dimer					
S_1S_1/CT	$1^1B_{2u} \otimes 1^1B_{2u}$	6.55	60.1	31.5	3.36
CT/S_1S_1	$1^1B_{2u} \otimes 1^1B_{2u}$	6.68	35.5	62.6	2.83
S_1S_2 (1)	$1^1B_{2u} \otimes 1^1B_{3u}$	6.84	97.9	1.6	4.06
S_1S_2 (2)	$1^1B_{2u} \otimes 1^1B_{3u}$	6.86	82.4	14.1	3.89
S_2S_2	$1^1B_{3u} \otimes 1^1B_{3u}$	7.07	97.1	2.7	4.05

[a]See the Supporting Information for computational details. (+) and (−) indicate in-phase and out-of-phase combinations of monomeric states, respectively, while (1) and (2) correspond to well-defined exciton states for each monomer.

to take into account the possible effects of dynamical correlation (see the Supporting Information for details).

Short intermolecular distance induces stronger excitonic coupling that favors the contribution of CT excitations to the ME wave function of *SS* states. As a result, *SS* states in the diagonal dimer present systematically a larger participation of ionic configurations, while in the parallel pair the potential BF precursors are almost purely ME states obtained as the product of two singlet monomer excitons. Moreover, the non-equivalence between monomers plays a very important role in shaping the properties of electronic states in the diagonal case. The difference between the two pairs becomes evident by comparing the qualitative energy diagram of their frontier orbitals (Figure S7).

The lowest *SS* state for the two dimers mainly corresponds to the direct product of two 1^1B_{2u} states (S_1S_1). In the parallel disposition this is obtained as a symmetric exciton combination with small intermolecular CT (∼1%). The CT contributions cancel each other out resulting in no net electron transfer between the two chromophores, i.e. charge resonances. On the other hand, in the diagonal dimer CT accounts for more than 30% of the wave function, corresponding to electronic transfer from molecule B to molecule A (Figure 2). The different nature of S_1S_1 in the two dimers is also reflected in the amount of unpaired electrons measured by the Head-Gordon index[73] in Table 1. In the diagonal pair, there is another state with strong ME character. It corresponds to a B → A electron transfer (62%) mixed with S_1S_1 (33%) and computed 0.13 eV higher than the lowest *SS* state. The S_1S_2 states appear in both cases within the 6.84−6.86 eV excitation energy range. The small energy splitting between the two states (∼0.01 eV) is an indication of weak excitonic coupling. In the parallel dimer the two states correspond to the in-phase (+) and out-of-phase (−) combinations of the 1^1B_{2u} and 1^1B_{3u} molecular states, while in the diagonal dimer the two states are the product of 1^1B_{2u} and 1^1B_{3u} in molecules A and B, respectively, in S_1S_2 (1) and its counterpart in S_1S_2 (2). Again, CT contributions are larger in the diagonal case, in particular in S_1S_2 (2), where the B → A electron transfer accounts for more than 13% of the wave function. The concomitant excitation to the 1^1B_{3u} state on the two monomers is computed at 7.1 eV. The obtained transition

Figure 4. Norm of the one-particle transition density matrix (γ) between the lowest *SS* states, S_1S_1 (left), S_1S_2 (middle), and S_2S_2 (right) and electronic excited singlet states (X) within the 3 to 8 eV excitation energies for the parallel (top) and diagonal (bottom) anthracene dimers. The X states are classified as local excitons (LE, red), charge resonance or charge transfer states (CR/CT, blue), and singlet−singlet (SS, green) and triplet−triplet (TT, black) multiexcitons.

energy is virtually the same in both dimer structures, which is an indication of weak exciton interaction between 1^1B_{3u} states on each of the molecules. The S_2S_2 state in both dimers is mainly of the ME nature, with slightly larger CT in the diagonal case, also corresponding to B → A electron transitions.

The rate of population and depopulation of the BF precursors via nonadiabatic transition from or to energetically close singlet states is related to their NAC. Here I use the norm of the one-particle transition density matrix[74] (γ) as an approximation to NAC in the anthracene dimers (Supporting Information), as it has been recently done for the study of SF in tetracene and pentacene dimers.[75]

Figure 4 shows the computed γ values for the NAC constants of the S_1S_1, S_2S_2, and the lowest S_1S_2 states with singlet states within the 3 to 8 eV excitation energy range. Like in the case of dipole−dipole Coulomb couplings of S_0S_n to singlet excited states (Figure 3), the γ values are in general larger in the diagonal dimer than in the parallel pair. The largest γ values for S_1S_1 and S_2S_2 are obtained with S_0S_1 and S_0S_2, respectively, while S_1S_2 shows large values to both lowest-lying local excitons (LE). With the exception of S_0S_1 and S_0S_2, charge transfer and/ or charge resonance states have in general larger γ to S_iS_j states than LE. In general, there is more than a single electron involved in the transition between *SS* and spin-singlet coupled triplet states (*TT*), resulting in small γ values. The coupling between *SS* states is rather high ($0.50 < \gamma < 0.75$). It is also important to remember that these states are relatively close in

energy (Table 1). Thus, once the singlet−singlet manifold is reached the system is expected to rapidly relax to the lowest *SS*. This would suggest that the fission is most probably occurring from S_1S_1.

3.3. Delocalization of Optical Excitons. At this point, it is important to emphasize that excitonic states in organic molecular crystals are expected to expand over several chromophoric units.[76] Exciton delocalization might have some impact on the electronic coupling between states and could be a key factor on the availability of different deactivation pathways like the BF process. Hence, the results obtained in the previous sections based on molecular and dimeric models, respectively, must be taken with caution and mainly as qualitative approximations. This is particularly important when dealing with high-energy excitons such as the optical S_n states, which normally exhibit even larger spatial delocalization degrees than the low-lying transitions.

In order to qualitatively investigate the possible spatial extend of the high-energy optical states, I have performed an analysis of the natural transition orbitals (NTOs) of dipole allowed electronic transitions in anthracene clusters. Here I focus on the lowest singlet exciton derived from the 8^1B_{2u} optical state of the monomer, that is the lowest state with sizable couplings to the *SS* manifold, for a molecular cluster with ten anthracene molecules (Figure 5). Results presented in this section were obtained with the long-range corrected ωB97X-D energy functional[77] and the 6-31G basis set. Exciton localization
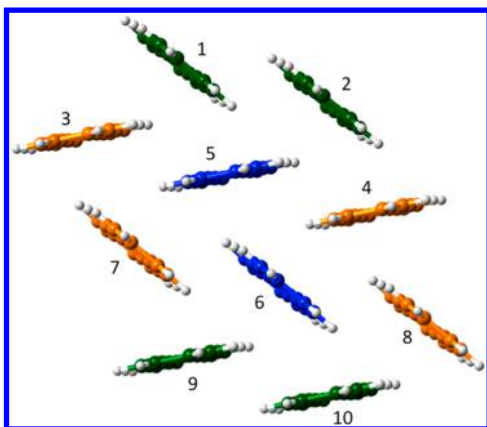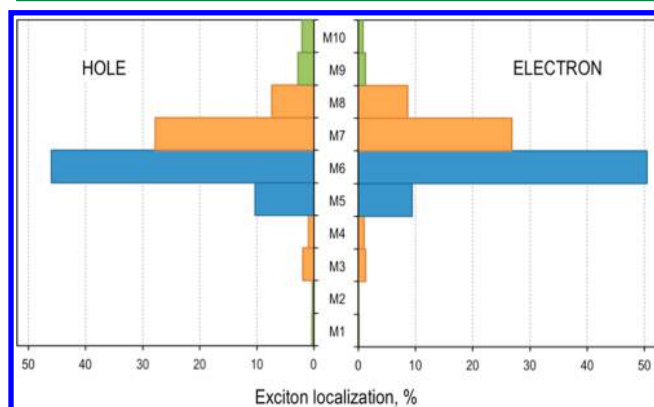
Figure 5. Cluster with ten molecules from the crystal structure of anthracene. Colors are used to better distinguish the monomers.

analysis for other states and clusters can be found as Supporting Information (Figures S2, S3, and S4).

Figure 6 shows the localization distribution of the hole and electron for the lowest singlet state of the anthracene cluster

Figure 6. Localization of the hole (left) and electron (right) for the lowest exciton of the cluster with 10 anthracene molecules (M1–M10) defined in Figure 5. The hole/electron percentage of the exciton on each monomer is obtained through NTO analysis at the ωB97X-D/6-31G level.

derived from the 8^1B_{2u} molecular excitation. In this case, the electron–hole pair is localized considerably on one anthracene molecule, that is ~50% of the transition takes place within one of the two central monomers of the aggregate (monomer 6). Contributions from one of its first molecular neighbors, that is monomer 7, account for almost 30% of the exciton hole and electron. The rest of the exciton mainly delocalizes over two other first neighbor anthracene molecules. Overall, more than 90% of the electron–hole pair is contained within four chromophores. Contributions from other anthracene molecules of the cluster, i.e. monomers 1–4 and 9–10, are negligible.

The fact that, for the most part, the excitonic state remains on one or two molecular species seems to validate the dimer approach employed in the previous sections, at least qualitatively. Similar results are also obtained for other high-lying states and for other anthracene clusters (Figures S3 and S4). Excitonic delocalization on a few anthracene molecules might be advantageous in order to promote the transit from the S_n state to the SS manifold, increasing their NACs. Higher delocalization of the electron–hole pair could decrease the BF

feasibility. In that case, BF could require efficient exciton localization from the initial delocalized exciton.

4. FINAL REMARKS AND PERSPECTIVES

In this work I have introduced and discussed the BF photophysical process, that is the singlet exciton fission into two singlet states in organic materials.

The present paper explores the theoretical foundations of BF regarding the nature of appropriate electronic states and mechanisms, competing deactivation channels, and the requirements for BF chromophores and their electronic couplings necessary for its feasibility. The study has identified possible high-lying optical states as good candidates to trigger the BF mechanism through their nonradiative conversion to energetically close singlet–singlet composite states in crystal anthracene. The diagonal dimer exhibits a larger number of direct transitions from the initially excited state to the SS manifold, especially in the domain close to the excitation frequencies. Exciton transitions to SS states in the parallel dimer are predicted to contribute at larger excitation energies than in the diagonal pair. The study also presents an electronic structure characterization of the lowest-lying SS states as BF precursors. The analysis of the electronic wave function of the S_1S_1 state reveals important electronic structure differences between the diagonal and parallel dimers, with larger CT contributions in the former. The norm of one-particle transition density matrices indicates possible large NAC of S_iS_j states to the lowest S_0S_i local excitons, for several CT states, especially those of the diagonal pair. The values between SS states seem to indicate a fast downhill nonadiabatic transition to the S_1S_1 state within the manifold of ME singlet–singlet states. Finally, the delocalization of the high-energy optical excitons has been investigated for a moderately large molecular cluster. The results obtained suggest that the electron–hole pair for these excitations extend over a few anthracene molecules.

This account is aimed at being a starting point for future studies on BF mechanism and its availability, both at theoretical and experimental levels. Nonetheless, it is worth emphasizing that one bold step in this direction should be to reproduce and confirm the results reported by Klein and Voltz of BF measurements in anthracene crystals, for they constitute up to date the sole experimental evidence of bright fission.

■ ASSOCIATED CONTENT

Ⓢ Supporting Information

Computational details, discussion of electronic states of the anthracene molecule (Table S1 and Figure S1), symmetry and exciton couplings in anthracene dimers, norm of the one particle transition density matrix, additional figures (Figures S2, S3, and S4) and references. The Supporting Information is available free of charge on the ACS Publications website at DOI: 10.1021/acs.jctc.5b00144.

■ AUTHOR INFORMATION

Corresponding Author
*E-mail: david.casanova@ehu.es.

Notes
The authors declare no competing financial interest.

■ ACKNOWLEDGMENTS

■ REFERENCES

(1) Smith, M. B.; Michl, J. *Chem. Rev.* **2010**, *110*, 6891.

(2) Smith, M. B.; Michl, J. *Annu. Rev. Phys. Chem.* **2013**, *64*, 361.

(3) Singh, S.; Jones, W. J.; Siebrand, W.; Stoicheff, B. P.; Schneider, W. G. *J. Chem. Phys.* **1965**, *42*, 330.

(4) Nozik, A. J.; Ellingson, R. J.; Mićić, O. I.; Blackburn, J. L.; Yu, P.; Murphy, J. E.; Beard, M. C.; Rumbles, G. In *Twenty-Seventh DOE Solar Photochemistry Research Conference*; Warrenton, Virginia, 2004; p 63.

(5) Shockley, W.; Queisser, H. J. *J. Appl. Phys.* **1961**, *32*, 510.

(6) Aryanpour, K.; Muñoz, J. A.; Mazumdar, S. *J. Phys. Chem. C* **2013**, *117*, 4971.

(7) Ehrler, B.; Wilson, M. W. B.; Rao, A.; Friend, R. H.; Greenham, N. C. *Nano Lett.* **2012**, *12*, 1053.

(8) Jadhav, P. J.; Brown, P. R.; Thompson, N.; Wunsch, B.; Mohanty, A.; Yost, S. R.; Hontz, E.; Van Voorhis, T.; Bawendi, M. G.; Bulović, V.; Baldo, M. A. *Adv. Mater.* **2012**, *24*, 6169.

(9) Lee, J.; Jadhav, P.; Reusswig, P. D.; Yost, S. R.; Thompson, N. J.; Congreve, D. N.; Hontz, E.; Van Voorhis, T.; Baldo, M. A. *Acc. Chem. Res.* **2013**, *46*, 1300.

(10) Thompson, N. J.; Hontz, E.; Congreve, D. N.; Bahlke, M. E.; Reineke, S.; Van Voorhis, T.; Baldo, M. A. *Adv. Mater.* **2014**, *26*, 1366.

(11) Yost, S. R.; Lee, J.; Wilson, M. W. B.; Wu, T.; McMahon, D. P.; Parkhurst, R. R.; Thompson, N. J.; Congreve, D. N.; Rao, A.; Johnson, K.; Sfeir, M. Y.; Bawendi, M. G.; Swager, T. M.; Friend, R. H.; Baldo, M. A.; Van Voorhis, T. *Nat. Chem.* **2014**, *6*, 492.

(12) Zeng, T.; Ananth, N.; Hoffmann, R. *J. Am. Chem. Soc.* **2014**, *136*, 12638.

(13) Ehrler, B.; Walker, B. J.; Böhm, M. L.; Wilson, M. W. B.; Vaynzof, Y.; Friend, R. H.; Greenham, N. C. *Nat. Commun.* **2012**, *3*, 1019.

(14) Paci, I.; Johnson, J. C.; Chen, X.; Rana, G.; Popović, D.; David, D. E.; Nozik, A. J.; Ratner, M. A.; Michl, J. *J. Am. Chem. Soc.* **2006**, *128*, 16546.

(15) Reusswig, P. D.; Congreve, D. N.; Thompson, N. J.; Baldo, M. A. *Appl. Phys. Lett.* **2012**, *101*, 113304.

(16) Chan, W.-L.; Tritsch, J. R.; Zhu, X. Y. *J. Am. Chem. Soc.* **2012**, *134*, 18295.

(17) Lee, J.; Bruzek, M. J.; Thompson, N. J.; Sfeir, M. Y.; Anthony, J. E.; Baldo, M. A. *Adv. Mater.* **2013**, *25*, 1445.

(18) Schwerin, A. F.; Johnson, J. C.; Smith, M. B.; Sreearunothai, P.; Popović, D.; Černý, J.; Havlas, Z.; Paci, I.; Akdag, A.; MacLeod, M. K.; Chen, X.; David, D. E.; Ratner, M. A.; Miller, J. R.; Nozik, A. J.; Michl, J. *J. Phys. Chem. A* **2010**, *114*, 1457.

(19) Ramanan, C.; Smeigh, A. L.; Anthony, J. E.; Marks, T. J.; Wasielewski, M. R. *J. Am. Chem. Soc.* **2011**, *134*, 386.

(20) Müller, A. M.; Avlasevich, Y. S.; Schoeller, W. W.; Müllen, K.; Bardeen, C. J. *J. Am. Chem. Soc.* **2007**, *129*, 14240.

(21) Johnson, J. C.; Akdag, A.; Zamadar, M.; Chen, X.; Schwerin, A. F.; Paci, I.; Smith, M. B.; Havlas, Z.; Miller, J. R.; Ratner, M. A.; Nozik, A. J.; Michl, J. *J. Phys. Chem. B* **2013**, *117*, 4680.

(22) Nichols, V. M.; Rodriguez, M. T.; Piland, G. B.; Tham, F.; Nesterov, V. N.; Youngblood, W. J.; Bardeen, C. J. *J. Phys. Chem. C* **2013**, *117*, 16802.

(23) Eaton, S. W.; Shoer, L. E.; Karlen, S. D.; Dyar, S. M.; Margulies, E. A.; Veldkamp, B. S.; Ramanan, C.; Hartzler, D. A.; Savikhin, S.; Marks, T. J.; Wasielewski, M. R. *J. Am. Chem. Soc.* **2013**, *135*, 14701.

(24) Roberts, S. T.; McAnally, R. E.; Mastron, J. N.; Webber, D. H.; Whited, M. T.; Brutchey, R. L.; Thompson, M. E.; Bradforth, S. E. *J. Am. Chem. Soc.* **2012**, *134*, 6388.

(25) Wang, C.; Angelella, M.; Kuo, C.-H.; Tauber, M. J. In *SPIE Proceedings*; 2012; Vol. *8459*, p 845905.

(26) Wang, C.; Tauber, M. J. *J. Am. Chem. Soc.* **2010**, *132*, 13988.

(27) Dillon, R. J.; Piland, G. B.; Bardeen, C. J. *J. Am. Chem. Soc.* **2013**, *135*, 17278.

(28) Thorsmølle, V. K.; Averitt, R. D.; Demsar, J.; Smith, D. L.; Tretiak, S.; Martin, R. L.; Chi, X.; Crone, B. K.; Ramirez, A. P.; Taylor, A. J. *Phys. Rev. Lett.* **2009**, *102*, 017401.

(29) Wilson, M. W. B.; Rao, A.; Johnson, K.; Gélinas, S.; di Pietro, R.; Clark, J.; Friend, R. H. *J. Am. Chem. Soc.* **2013**, *135*, 16680.

(30) Johnson, J. C.; Nozik, A. J.; Michl, J. *J. Am. Chem. Soc.* **2010**, *132*, 16302.

(31) Chan, W.-L.; Berkelbach, T. C.; Provorse, M. R.; Monahan, N. R.; Tritsch, J. R.; Hybertsen, M. S.; Reichman, D. R.; Gao, J.; Zhu, X. Y. *Acc. Chem. Res.* **2013**, *46*, 1321.

(32) Thorsmølle, V. K.; Averitt, R. D.; Demsar, J.; Smith, D. L.; Tretiak, S.; Martin, R. L.; Chi, X.; Crone, B. K.; Ramirez, A. P.; Taylor, A. J. *Physica B* **2009**, *404*, 3127.

(33) Schrauben, J. N.; Ryerson, J. L.; Michl, J.; Johnson, J. C. *J. Am. Chem. Soc.* **2014**, *136*, 7363.

(34) Wu, Y.; Liu, K.; Liu, H.; Zhang, Y.; Zhang, H.; Yao, J.; Fu, H. *J. Phys. Chem. Lett.* **2014**, *5*, 3451.

(35) Chan, W.-L.; Ligges, M.; Zhu, X. Y. *Nat. Chem.* **2012**, *4*, 840.

(36) Jadhav, P. J.; Mohanty, A.; Sussman, J.; Lee, J.; Baldo, M. A. *Nano Lett.* **2011**, *11*, 1495.

(37) Congreve, D. N.; Lee, J.; Thompson, N. J.; Hontz, E.; Yost, S. R.; Reusswig, P. D.; Bahlke, M. E.; Reineke, S.; Van Voorhis, T.; Baldo, M. A. *Science* **2013**, *340*, 334.

(38) Ito, S.; Minami, T.; Nakano, M. *J. Phys. Chem. C* **2012**, *116*, 19729.

(39) Greyson, E. C.; Vura-Weis, J.; Michl, J.; Ratner, M. A. *J. Phys. Chem. B* **2010**, *114*, 14168.

(40) Zeng, T.; Hoffmann, R.; Ananth, N. *J. Am. Chem. Soc.* **2014**, *136*, 5755.

(41) Minami, T.; Ito, S.; Nakano, M. *J. Phys. Chem. Lett.* **2012**, *3*, 2719.

(42) Havenith, R. W. A.; de Gier, H. D.; Broer, R. *Mol. Phys.* **2012**, *110*, 2445.

(43) Johnson, J. C.; Nozik, A. J.; Michl, J. *Acc. Chem. Res.* **2013**, *46*, 1290.

(44) Casanova, D. *J. Chem. Theory Comput.* **2013**, *10*, 324.

(45) Zimmerman, P. M.; Musgrave, C. B.; Head-Gordon, M. *Acc. Chem. Res.* **2013**, *46*, 1339.

(46) Beljonne, D.; Yamagata, H.; Brédas, J. L.; Spano, F. C.; Olivier, Y. *Phys. Rev. Lett.* **2013**, *110*, 226402.

(47) Zimmerman, P. M.; Bell, F.; Casanova, D.; Head-Gordon, M. *J. Am. Chem. Soc.* **2011**, *133*, 19944.

(48) Berkelbach, T. C.; Hybertsen, M. S.; Reichman, D. R. *J. Chem. Phys.* **2013**, *138*, 114102.

(49) Feng, X.; Kolomeisky, A. B.; Krylov, A. I. *J. Phys. Chem. C* **2014**, *118*, 19608.

(50) Kolomeisky, A. B.; Feng, X.; Krylov, A. I. *J. Phys. Chem. C* **2014**, *118*, 5188.

(51) Renaud, N.; Sherratt, P. A.; Ratner, M. A. *J. Phys. Chem. Lett.* **2013**, *4*, 1065.

(52) Teichen, P. E.; Eaves, J. D. *J. Phys. Chem. B* **2012**, *116*, 11473.

(53) Wegh, R. T.; Donker, H.; Oskam, K. D.; Meijerink, A. *Science* **1999**, *283*, 663.

(54) Zhang, Q. Y.; Huang, X. Y. *Prog. Mater. Sci.* **2010**, *55*, 353.

(55) Richards, B. S. *Sol. Energy Mater. Sol. Cells* **2006**, *90*, 2329.

(56) Wegh, R. T.; Donker, H.; van Loef, E. V. D.; Oskam, K. D.; Meijerink, A. *J. Lumin.* **2000**, *87–89*, 1017.

(57) Klein, G.; Voltz, R. *Int. J. Radiat. Phys. Chem.* **1975**, *7*, 155.

(58) Pope, M.; Swenberg, C. E. *Electronic Processes in Organic Crystals and Polymers*; Oxford University Press: New York, 1999.

(59) Silinsh, E. A.; Čápek, V. *Organic Molecular Crystals*; AIP Press: New York, 1994.

(60) Burdett, J. J.; Piland, G. B.; Bardeen, C. J. *Chem. Phys. Lett.* **2013**, *585*, 1.

(61) Northrop, D. C.; Simpson, O. *Proc. R. Soc. London, Ser. A* **1958**, *244*, 377.

(62) Pope, M.; Kallmann, H.; Giachino, J. *J. Chem. Phys.* **1965**, *42*, 2540.

(63) Kasha, M. *Discuss. Faraday Soc.* **1950**, *9*, 14.

(64) Lias, S. G. In *NIST Chemistry WebBook, NIST Standard Reference Database Number 69*; Linstrom, P. J., Mallard, W. G., Eds.; National Institute of Standards and Technology: Gaithersburg, MD, 20899, 2014.

(65) Birks, J. B. *Photophysics of Aromatic Molecules*; John Wiley & Sons Ltd.: Chichester, 1970.

(66) Klessinger, M.; Michl, J. *Excited States and Photochemistry of Organic Molecules*; VCH Publishers: New York, 1995.

(67) Zhao, Y.; Truhlar, D. *Theor. Chem. Acc.* **2008**, *120*, 215.

(68) Bixon, M.; Jortner, J. *J. Chem. Phys.* **1968**, *48*, 715.

(69) May, V.; Kühn, O. *Charge and Energy Transfer Dynamics in Molecular Systems*; Wiley-VCH: Berlin, 2000.

(70) Casanova, D.; Head-Gordon, M. *Phys. Chem. Chem. Phys.* **2009**, *11*, 9779.

(71) Casanova, D. *J. Chem. Phys.* **2012**, *137*, 084105.

(72) Casanova, D. *J. Comput. Chem.* **2013**, *34*, 720.

(73) Head-Gordon, M. *Chem. Phys. Lett.* **2003**, *372*, 508.

(74) Matsika, S.; Feng, X.; Luzanov, A. V.; Krylov, A. I. *J. Phys. Chem. A* **2014**, *118*, 11943.

(75) Feng, X.; Luzanov, A. V.; Krylov, A. I. *J. Phys. Chem. Lett.* **2013**, *4*, 3845.

(76) Lim, S.-H.; Bjorklund, T. G.; Spano, F. C.; Bardeen, C. J. *Phys. Rev. Lett.* **2004**, *92*, 107402.

(77) Chai, J.-D.; Head-Gordon, M. *Phys. Chem. Chem. Phys.* **2008**, *10*, 6615.